Possible assignment of chiral twin bands in ^{188}Ir

D. L. Balabanski,[1,2,*] M. Danchev,[1,2] D. J. Hartley,[1,†] L. L. Riedinger,[1,3] O. Zeidan,[1] Jing-ye Zhang,[1] C. J. Barton,[4] C. W. Beausang,[4] M. A. Caprio,[4] R. F. Casten,[4] J. R. Cooper,[4] A. A. Hecht,[4] R. Krücken,[4,‡] J. R. Novak,[4] N. V. Zamfir,[4,5,6] and K. E. Zyromski[4]

[1]*Department of Physics and Astronomy, University of Tennessee, Knoxville, Tennessee 37996, USA*
[2]*Faculty of Physics, St. Kliment Ohridski University of Sofia, BG-1164 Sofia, Bulgaria*
[3]*Oak Ridge National Laboratory, Oak Ridge, Tennessee 37831, USA*
[4]*WNSL, Physics Department, Yale University, New Haven, Connecticut 06520, USA*
[5]*Clark University, Worcester, Massachusetts 10610, USA*
[6]*National Institute for Physics and Nuclear Engineering, Bucharest-Magurele, Romania*

(Received 14 September 2003; revised manuscript received 28 April 2004; published 11 October 2004)

High-spin states in the doubly-odd $Z=77$ nucleus ^{188}Ir were populated in the ^{186}W(^{7}Li,$5n$) reaction at 52 MeV. Two nearly degenerate $\Delta I=1$ sequences with the same parity were established. Both bands have been assigned the $\pi h_{9/2} \otimes \nu i_{13/2}$ configuration, based on the systematic behavior of these excitations in the Ir nuclei and on the measured values for the $B(M1)/B(E2)$ ratios, and they are suggested as candidates for a chiral doublet.

DOI: 10.1103/PhysRevC.70.044305 PACS number(s): 21.60.Ev, 21.60.Fw, 23.20.Lv, 27.70.+q

I. INTRODUCTION

Chirality is a recently introduced symmetry of nuclear rotation [1]. Using the tilted axis cranking (TAC) model [2], it has been shown in Refs. [3,4] that the rotating mean field of triaxial nuclei can break chiral symmetry. Experimentally this led to observation of two nearly degenerate $\Delta I=1$ bands of the same parity, which are called chiral twin bands.

Chiral symmetry can be broken for a triaxial doubly-odd nucleus with substantial γ deformation, for which the proton (neutron) Fermi level is located in the lower part of a high-j subshell, while the neutron (proton) Fermi level is located in the upper part of a high-j subshell [5]. The latter particle might be considered as a valence hole in the high-j subshell. The angular momentum of the valence particle $\mathbf{j}_\pi$ ($\mathbf{j}_\nu$), is then aligned along the short axis, and that of the valence hole $\mathbf{j}_\nu$ ($\mathbf{j}_\pi$) along the long axis [6]. In the limit of uniform rotation of an irrotational-like and incompressible liquid [7], the core angular momentum vector $\mathbf{R}$ aligns along the intermediate axis, as it possesses the largest moment of inertia. Such a coupling of both the valence particle and the hole with the triaxial core minimizes the interaction energy of the system. These three mutually perpendicular angular momenta: of the valence particle, hole, and of the triaxial core, $\mathbf{j}_\pi$, $\mathbf{j}_\nu$, and $\mathbf{R}$, form either a left-handed or right-handed coordinate system. Consequently total angular momentum $\mathbf{I}$ chooses one of the systems, thus introducing chirality.

It has been suggested that chiral twin bands might be observed in the $A\sim 130$ and $A\sim 190$ transitional regions [1] and consequently the existence of chiral solutions for these two regions was demonstrated in the Ref. [3]. A well developed $\Delta I=1$ sideband of the same parity as the yrast $\pi h_{11/2} \otimes \nu h_{11/2}$ band has been observed first in ^{134}Pr [8], and later on a chiral interpretation has been suggested for these two bands [1]. Chiral twin bands, which are built on the $\pi h_{11/2} \otimes \nu h_{11/2}$ configuration, has been established recently in several doubly odd $N=73$, 75, 77 $_{55}$Cs, $_{57}$La, $_{59}$Pr, $_{61}$Pm, and $_{63}$Eu nuclei [5,9–15]. In all these cases the observed mixed $M1/E2$ linking transitions between the two nearly degenerate bands of the same parity and the similar ratios of the reduced transitions probabilities in both bands have been considered as the experimental evidence, which reflects their common underlying structure.

In the ideal case of strongly broken chiral symmetry the chiral twin bands should be degenerate. In reality, for all known cases the twin bands separate from each other [5,9–15]. When the triaxial core deformation is not stable with respect to γ deformation the total angular momentum $\mathbf{I}$ is not constrained to one of the left- or right-handed systems of different chirality and therefore can oscillate from one system to the other. This mechanism, called chiral vibration has been suggested to account for the almost constant separation between the twin bands, observed in the $N=75$ $A\sim 130$ doubly odd nuclei [5,16].

Studies on nuclear chirality were focused so far on the mass $A\sim 130$ region, but there is no reason to consider the mass $A\sim 130$ nuclei unique in terms of the underlying physics, and it is therefore necessary to look for other examples in the $A\sim 190$ region, where chirality also can be observed. Following this motivation we have studied the high-spin states of $^{188}_{77}\mathrm{Ir}_{111}$. The Ir nuclei has 77 protons and lie in the transitional region between the well deformed rare-earth nuclei and the spherical nuclei near doubly magic $^{208}_{82}$Pb. Depending on the neutron number, nuclear deformation in this region may vary between prolate, oblate and triaxial. These large shape variations are also indication that the cores of

*Present address: Dipartimento di Fisica, Università degli Studi di Camerino, 62032 Camerino (MC), Italy.
†Present address: Department of Physics, United States Naval Academy, Annapolis, MD 21402, U.S.A.
‡Present address: Physik-Department E12, Technische Universität München, 85748 Garching, Germany.

these nuclei are "soft" with respect to γ deformation. For example, theoretical calculations for the odd-A $_{78}$Pt nuclei, yield a smooth shape transition from a strongly deformed prolate ^{185}Pt via triaxial $^{187-193}$Pt to a slightly deformed oblate ^{195}Pt [17]. Such transition is expected to occur also for the $_{77}$Ir nuclei. The proton Fermi level is located in lower part of both, the $\pi h_{9/2}$ and $\pi i_{13/2}$ subshells, while it is located in the upper part of the $\pi h_{11/2}$ subshell. The neutron Fermi level is located in the upper part of the $\nu i_{13/2}$ subshell. The γ softness of these nuclei means that the deformation may be greatly influenced by the properties of specific single-particle wave functions. For example, in ^{186}Ir a difference in the deformation of the 5^+ ground state ($\beta=+0.23$) and the low-lying 2^- isomer ($\beta=+0.17$) has been found [18]. The enhancement of the deformation for the ground state is a result of the $\pi\frac{1}{2}^-[541]$ intruder orbital, which is present in the configuration.

Here we report the first experimental evidence for chiral rotation in a mass $A\sim 190$ region. Two nearly degenerate $\Delta I=1$ sequences have been established in ^{188}Ir, which have been assigned same $\pi h_{9/2}\otimes\nu i_{13/2}$ configuration and they are suggested as candidates for a chiral doublet. The details of the experiments and the experimental results are presented in Sec. II. The results are discussed in Sec. III.

II. EXPERIMENTAL DETAILS AND RESULTS

The ^{186}W(^{7}Li,$5n$) reaction at 52 MeV was utilized to populate the high-spin states in ^{188}Ir. The ^{7}Li beam was delivered by the ESTU Tandem van de Graff accelerator at the Wright Nuclear Structure Laboratory at Yale University. The target consisted of three stacked foils of ^{186}W, each of thickness 0.3 mg/cm^2. Gamma rays were detected by the YRAST Ball array [19], which consisted of five clover detectors, 17 single-crystal Ge detectors, and four low-energy photon spectrometers (LEPS) detectors for this experiment. All clover detectors were located at 90°, three of the Ge single-crystal detectors were at 160°, eight at 126.5°, and the others at 50°. All coincident γ rays were sorted into the $E_\gamma-E_\gamma$ matrix and analyzed with the RADWARE package [20].

Prior to our experiment only the low-spin states in ^{188}Ir were known and no rotational bands were established [21]. The quadrupole moment of the 1^- ground state in ^{188}Ir also has been measured [18]. It is in agreement with the systematic measurements of the quadrupole moments of the $\frac{3}{2}^+$ states in the Ir and the Au nuclei, which supports the suggested $\pi\frac{3}{2}^+[402]\otimes\nu\frac{1}{2}^-[510]$ configuration for this state [21]; a discussion on the spin of this state is given in Ref. [22]. The low-spin part of the level scheme is built on this state. A millisecond isomer [$T_{1/2}=4.2(2)$ms] has been reported to decay to the low-spin states [21].

In the present study we have expanded the level scheme of ^{188}Ir considerably. Two $\Delta I=1$ bands were observed together with a number of single particle states. Since no γ rays connecting high-spin states were known, we measured γ-ray excitation functions at beam energies of 45, 49, 52, and 55 MeV. Along with the ^{188}Ir nucleus, the ^{187,189}Ir nuclei were also populated. These nuclei have well established high-spin levels [23]. The intensities of the strongest transitions observed in the total projection were deduced and plotted versus excitation energy after an appropriate normalization as shown in Fig. 1. The γ rays can be separated in three different groups with respect to their dependence on excitation energy. The excitation functions for the γ rays, which are known to belong to ^{187}Ir are displayed in the upper panel of Fig. 1. The intensity of these γ rays increase with the increase of the beam energy. The 263 keV γ ray, which is known to belong to ^{189}Ir (the $4n$ reaction channel), has a decreasing excitation function, as demonstrated in the lowest section of Fig. 1. In the middle part of Fig. 1 the excitation functions for a number of γ rays are shown. All of them have not been observed previously and have a different behavior compared to the γ rays associated with ^{189}Ir and ^{187}Ir (the $6n$ reaction channel). Therefore, we associate them with the γ decay of ^{188}Ir (the $5n$ reaction channel).

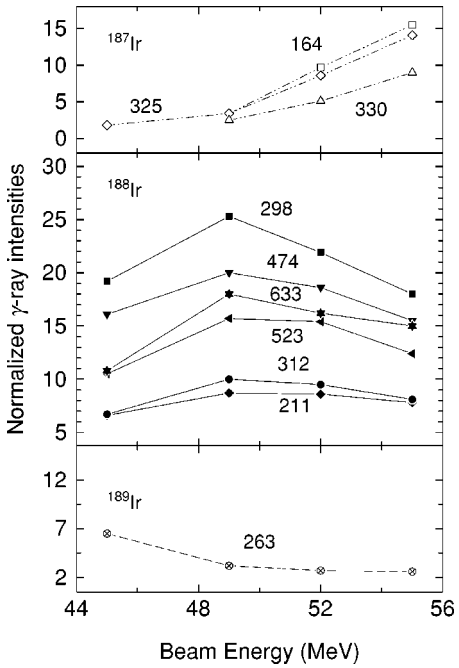

FIG. 1. Relative intensities of γ transitions at 45, 49, 52, and 55 keV energy of the ^{7}Li beam. The intensities were obtained from the total projection spectra and normalized to the total number of counts. Transitions with like behavior were separated in three different panels as follows: upper panel: transitions belonging to ^{187}Ir, middle panel: transitions assigned to ^{188}Ir, and lower panel: the 263 keV transition, which belongs to ^{189}Ir. The error bars of all measured intensities are of the order of the experimental points.

In order to deduce the multipolarity of the measured γ rays, the formalism of directional correlation from oriented states (DCO) was employed [24]. For this purpose an asymmetric matrix has been sorted by incrementing all events in which a coincidence between a γ ray detected at 90° and another one detected at 160° occurs. The DCO ratio is defined as

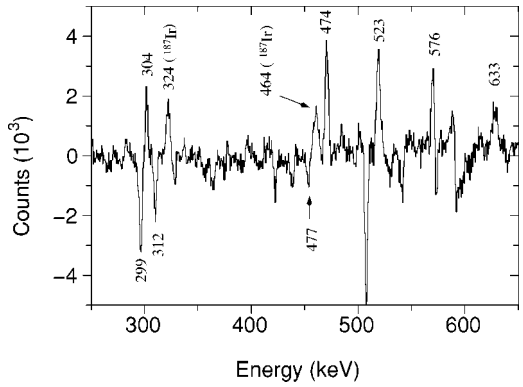

FIG. 2. Polarization spectrum revealing the multipolarity of the transitions. It has been obtained as a difference of total projections of γ rays detected in the clover detectors, which were scattered between perpendicular or parallel elements of the detector with respect to the reaction plane. The 324 and 464 keV γ rays belong to the yrast band in ^{187}Ir.

$$R_{\mathrm{DCO}} = \frac{I_{\gamma_1}^{160^\circ}(\text{in coincidence with } \gamma_2 \text{ at } 90^\circ)}{I_{\gamma_1}^{90^\circ}(\text{in coincidence with } \gamma_2 \text{ at } 160^\circ)}. \qquad (1)$$

For the present detector geometry a value of 0.51 is expected for pure dipole transitions ($E1$) and value of 1.0 for $E2$ transitions when the gating transition γ_2 is a stretched quadrupole transition. A value of 1.0 is expected for pure dipole transitions ($E1$) and value of 1.98 for $E2$ transitions when the gating transition γ_2 is a pure dipole transition ($E1$). We were also able to distinguish between magnetic (M) and electric (E) transitions by measuring the linear polarization of the γ rays using the five clover detectors as Compton polarimeters. Two spectra were sorted, the first of which contains all events which are scattered between the segments of the clover detectors, which were perpendicular to the reaction plane, while the other one contains all events scattered parallel to the reaction plane. The difference in these two spectra is shown in Fig. 2, as all electric transitions take positive values and all magnetic transitions take negative values.

The level scheme, which has been deduced from the present study is shown in Fig. 3. The assignment of γ rays is based on their coincidence relationship and the measured relative intensities. Information on all transitions assigned to ^{188}Ir are summarized in the Table I together with their intensities, DCO ratios and proposed multipolarities. Sample experimental spectra, revealing the transitions assigned to ^{188}Ir are displayed in Fig. 4.

Band 1 in Fig. 3 is the yrast sequence in ^{188}Ir. In a previous experiment, Kreiner *et al.* [21] used millisecond timing and reported only one delayed component [$T_{1/2}$=4.2(2)ms], which was observed for all low-spin transitions. They have suggested an isomer with an excitation energy 923.7 $+x$ keV and spin ranging from $I^\pi=(8^-)$ to $I^\pi=(11^-)$, which can be the bandhead of band 1. No γ rays have been observed to de-excite the bandhead. However, the existence of low-energy strongly converted transitions de-exciting the bandhead cannot be excluded completely. Therefore, the bandhead energy has been accepted to be 923.7+Δ keV, where $\Delta \geqslant 0$, as indicated in Fig. 3. Further, we provide arguments that this level has spin $I^\pi=9^-$. Three crossover transitions were found for each sequence of band 1. Intraband $\Delta I=1$ transitions were established throughout the band. Three $\Delta I=1$ transitions and three crossover transitions were established for band 2; the last of them being tentatively assigned (see Fig. 3). Band 2 decays to band 1 predominantly through the 457 keV transition. A DCO ratio R_{DCO} =0.92(12) was measured for this transition, which indicates an $M1/E2$ or a stretched $E2$ character. The linear polarization measurement indicates that this transition is a magnetic one, which supports the $M1/E2$ multipolarity (see Fig. 2). Thus, spin and parity $I^\pi=13^-$ are unambiguously assigned to the lowest level of band 2.

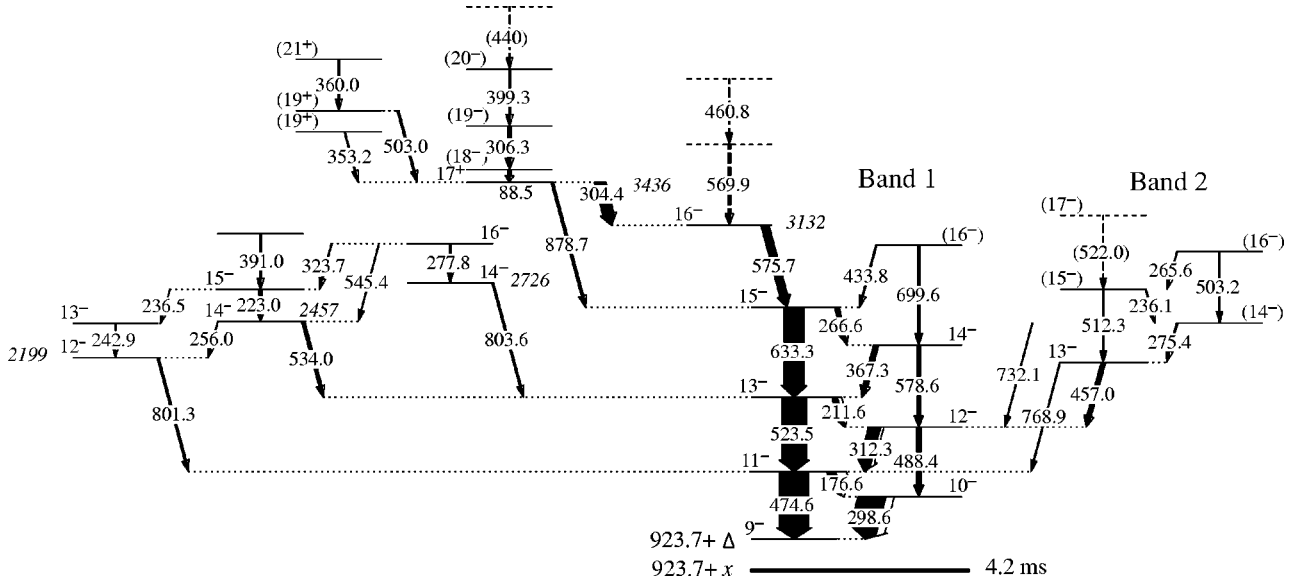

FIG. 3. Partial level scheme for ^{188}Ir showing the newly identified $\Delta I=1$ bands as populated in the ^{186}W(^{7}Li,5n) reaction at 54 MeV. Level spins are assigned under the assumption that spin of the 923.7+Δ level is 9^- (see discussion in the text).

TABLE I. Energies of γ rays assigned to ^{188}Ir, their relative intensities, DCO ratios, and multipolarities, as established in the ^{186}W(^{7}Li, 5n) reaction at 52 MeV.

E_γ (keV)	I_γ[a] (rel.)	$R_{dco}(Q)$[b]	$R_{dco}(D)$[c]	Assignment
		Band 1		
Odd spins				
176.6	29.4(9)	0.63(7)	0.76(7)	$M1/E2$
211.6	18.5(6)	0.76(9)	0.88(10)	$M1/E2$
266.6	10.6(4)	0.61(14)		$M1/E2$
474.6	100(3)	0.95(4)		$E2$
523.5	84(3)	0.97(4)	1.39(8)	$E2$
633.3	68(2)	1.06(6)	1.38(9)	$E2$
Even spins				
298.6	95(3)	0.66(3)	1.18(8)	$M1/E2$
312.3	41(1)	0.76(4)	0.95(7)	$M1/E2$
367.3	14.9(5)	0.59(7)	1.03(18)	$M1/E2$
433.8	3.5(2)			$(M1/E2)$
488.4	14.5(1)	1.34(22)	1.20(9)	$(E2)$
578.6	12.0(4)	0.63(31)	1.25(61)	$E2$
699.6	6.5(3)			$(E2)$
		Band 2		
236.1	2.6(2)	0.42(13)	0.74(19)	$(M1/E2)$
265.6	1.7(1)			$(M1/E2)$
275.4	3.6(2)			$(M1/E2)$
457.0	13.9(5)	0.92(12)	1.58(19)	$M1/E2$
503.2	1.6(2)	1.55(27)	1.56(29)	$(E2)$
512.3	3.9(2)			$(E2)$
522.0	2.3(2)			$(E2)$
732.1	2.4(2)			$(E2)$
768.9	2.8(2)			$(E2)$
		Other transitions		
88.5	6.8(3)	1.37(32)		$(E1)$
223.0	6.9(3)	0.75(11)	1.46(24)	$M1/E2$
236.5	1.3(1)	0.42(13)	0.74(19)	$M1/E2$
242.9	1.9(1)	0.43(15)		$M1/E2$
256.0	1.6(1)			$E2$
277.8	2.5(1)	1.06(20)		$E2$
304.4	38(1)	0.59(4)	0.80(7)	$E1$
306.3	9.0(3)	0.76(28)	0.70(37)	$(M1/E2)$
323.7	2.4(1)			$E2$
353.2	3.4(1)	0.98(27)		$(E2)$
360.0	3.9(2)	0.91(18)		$(E2)$
391.0	4.6(2)			
399.3	5.3(2)	1.3(3)		$(M1/E2)$
440.0	1.8(1)			
460.8	3.2(2)			
503.0	8.7(3)	1.16(20)		$(E2)$
534.0	10.0(4)	1.41(18)	1.43(21)	$M1/E2$
545.4	2.2(2)			$(E2)$
569.9	8.2(3)			
575.7	26.0(8)	1.22(6)	1.93(42)	$(M1/E2)$
801.3	6.3(4)	0.64(28)	0.35(10)	$M1/E2$
803.6	5.7(3)	0.30(17)	0.68(28)	$M1/E2$
878.7	7.6(3)	1.09(21)	1.93(60)	$(M2)$

[a]Relative γ-ray intensities normalized to 100% for the 474.6 keV transition.
[b]DCO ratio obtained by gating on a stretched quadrupole transition.
[c]DCO ratio obtained by gating on the 298.6 keV transition, which is a mixed $M1/E2$ transition.

The 4.2(2) ms isomer was previously assigned the $\pi h_{11/2} \otimes \nu i_{13/2}$ configuration, but it may also have the $\pi h_{9/2} \otimes \nu i_{13/2}$ configuration. The excitation energies of the $\pi h_{11/2}$ and $\pi h_{9/2}$ orbitals in the odd-A Ir nuclei are shown in Fig. 5. The energy of the $\pi h_{11/2}$ state decreases with the increase of neutron number, while that of the $\pi h_{9/2}$ state increases. The two curves cross between $A=187$ and $A=189$. The comparison of the experimental $B(M1)/B(E2)$ transition with the three-dimensional (3D)-TAC calculations discussed in Chap. III support the $\pi h_{9/2} \otimes \nu i_{13/2}$ configuration.

Bands which are built on the $\pi h_{9/2} \otimes \nu i_{13/2}$ configuration were observed for ^{184,186}Ir. In ^{184}Ir this is the ground-state $I^\pi, K=5^-, 5$ band [25,26], while in ^{186}Ir the lowest level observed in the band is $I^\pi=7^-$ at 312.9 keV [27]. The excitation energies *vs* spin of these bands, together with bands 1 and 2

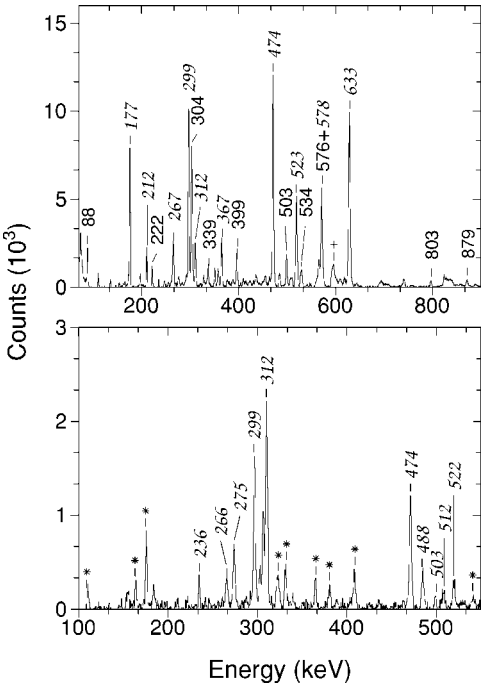

FIG. 4. Coincidence spectra, revealing the transitions for band 1 (upper panel) and band 2 (lower panel) in ^{188}Ir. The spectrum for band 1 is a sum of the 532 and 304 keV energy gates (the 304 keV transition feeds the band). The spectrum for band 2 is gated on the 457 keV transition, which depopulates the band. Contaminant transitions are denoted with an asterisk. In italic are indicated transitions belonging to bands 1 and 2.

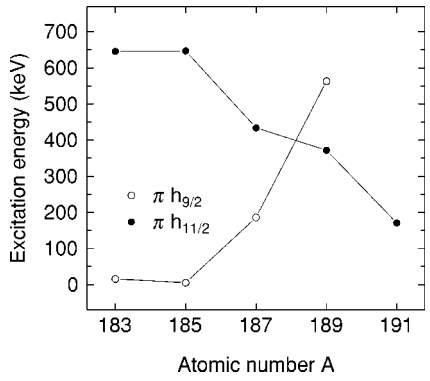

FIG. 5. Excitation energy with respect to the ground state of the $\pi h_{9/2}$ and $\pi h_{11/2}$ isomers in the odd-*A* Ir nuclei as a function of mass number.

in ^{188}Ir, are plotted in Fig. 6. Band 1 follows the same systematic pattern as the bands in the lighter Ir isotopes, which supports the assigned configuration. The plot also demonstrates that the initial displacement between the doublet bands in ^{188}Ir decreases when the spin increases.

The energy staggering of the $\pi h_{9/2} \otimes \nu i_{13/2}$ bands in the doubly odd Ir isotopes is shown in Fig. 7. Band 1 in ^{188}Ir displays the same phase of staggering like the other Ir isotopes if an odd spin for the bandhead is accepted. This reduce spin possibilities for band 1 to 9^- and 11^-, since the spin of the isomer was estimated to range from 8^- to 11^- as discussed earlier.

Taking into consideration the amplitude of the energy staggering we arrive at the conclusion that the bandhead spin $I^\pi = 9^-$ is the most probable. Support for adoption of this spin for the bandhead can also be derived from the systematic study of the excitation energies of the levels of the $\pi h_{9/2} \otimes \nu i_{13/2}$ bands in the doubly odd Ir nuclei. They are displayed in Fig. 8 relative to the $I^\pi = 9^-$ states assuming spin $I^\pi = 9^-$ for the $923.7 + \Delta$ keV level in ^{188}Ir. This results in a smooth increase of the excitation energy of the levels with the neutron number. Such behavior is expected as when the neutron number increases the neuron Fermi level moves away from the middle of the $N = 126$ neutron shell ($N = 104$). For a spin of $I^\pi = 11^-$ assumed for the $923.7 + \Delta$ keV level, excitation

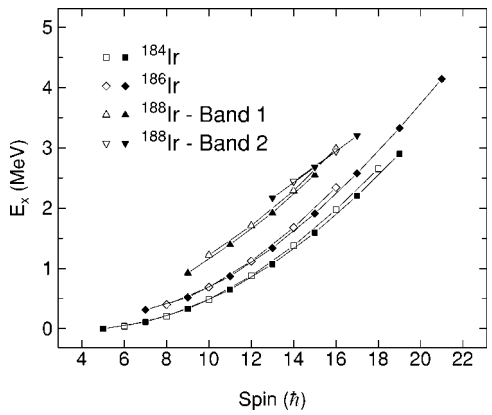

FIG. 6. Excitation energy vs spin for the $\pi h_{9/2} \otimes \nu i_{13/2}$ bands in ^{184,186}Ir, together with the $\Delta I = 1$ bands in ^{188}Ir.

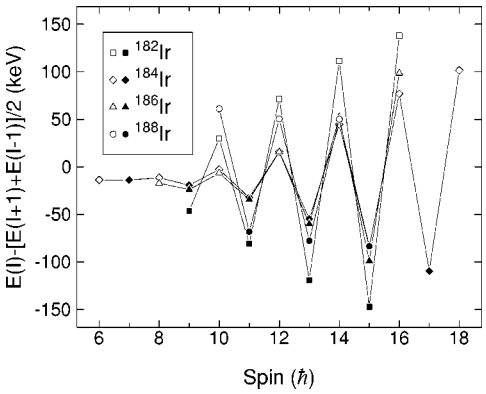

FIG. 7. Energy staggering of the $\pi h_{9/2} \otimes \nu i_{13/2}$ bands in the doubly odd Ir isotopes as a function of level spins.

energy trend will drop at ^{188}Ir. A spin of $I^\pi = 7^-$ or less for the bandhead will result in a very steep increase in excitation energy of the band at ^{188}Ir, which is rather unlikely.

In addition to bands 1 and 2 we have established a competing irregular structure of (most probably) single particle states, which decays to band 1. The excitation energy of the favored sequence of band 1 minus the energy of the rigid rotor, together with the energies of a few states from the irregular structure are plotted in Fig. 9. The pattern suggests that an abrupt band termination takes place [28]. Such competing single-particle structures have been observed in the doubly-odd ^{186}Ir, as well as in the neighboring odd-*A* Ir isotopes and will be discussed in detail in a forthcoming paper [29].

III. DISCUSSION

A total Routhian surface (TRS) calculation for the $\pi\left(-, +\frac{1}{2}\right) \otimes \nu\left(+, +\frac{1}{2}\right)$ configuration in ^{188}Ir at $\hbar\omega = 0.21$ MeV is presented in Fig. 10. It corresponds to the favored se-

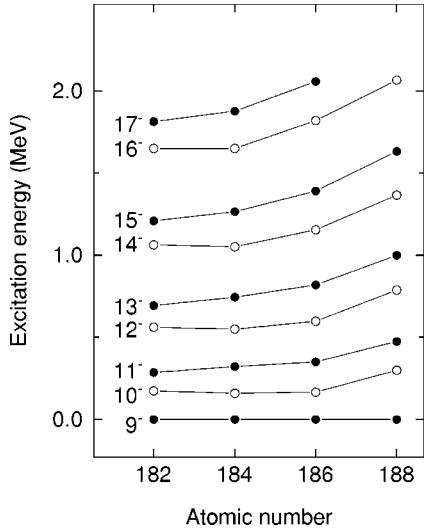

FIG. 8. Experimental excitation energies of the $\pi h_{9/2} \otimes \nu i_{13/2}$ band members relative to the 9^- state in the odd-odd Ir isotopes $^{182-188}$Ir. The bandhead spin of 9^- was accepted for band 1 in ^{188}Ir.

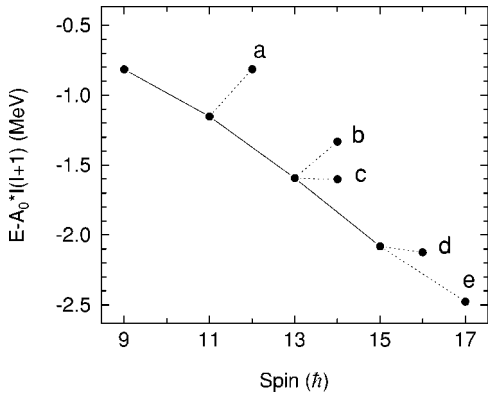

FIG. 9. The energy of the states belonging to the favorite signature of band 1 (minis a rigid rotor) vs spin. Labels from (a) to (e) on the figure correspond to the 2199, 2457, 2726, 3436 and 3132 keV levels. The parameter $A_0=0.0193$ was obtained from the ground state band in ^{186}Os.

quence of the $\pi h_{9/2}\otimes\nu i_{13/2}$ band and indicates that the triaxial shape stabilizes for this configuration at $\beta_2=0.17$, $\beta_4=0.04$, and $\gamma=-31°$. We have performed 3D-TAC calculations [30] for this configuration and the results are summarized in Table II. These calculations demonstrate the existence of an aplanar solution, having both θ and φ (the orientation angles for the spin axis) substantially different from 0° or 90°, i.e., outside the principal planes of the body-fixed reference frame and indicate that chiral rotation is possible for this configuration but only in a narrow frequency interval. It is because, aplanar solution can only exist while the core spin value is big enough and comparable with that

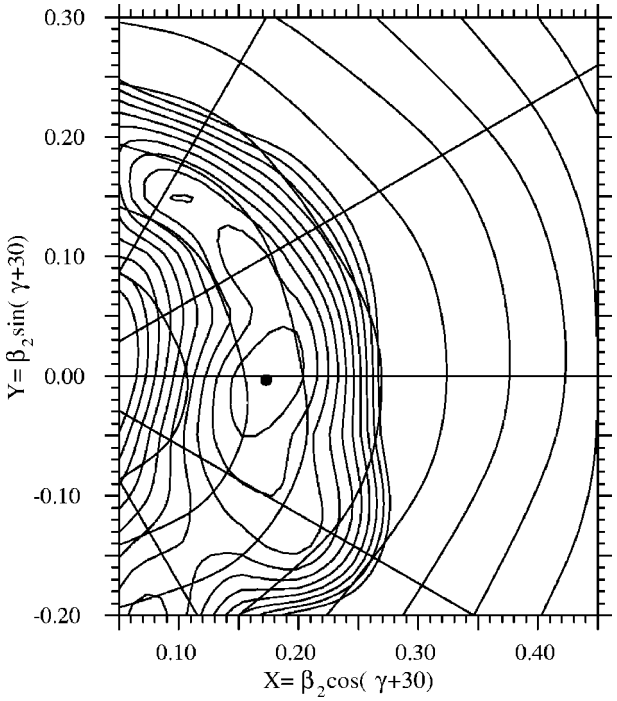

FIG. 10. Theoretical TRS calculation for the $\pi(-,+\frac{1}{2})\otimes\nu(+,+\frac{1}{2})$ configuration in ^{188}Ir at $\hbar\omega=0.21$ MeV. The equilibrium shape corresponds to $\gamma=-31°$.

TABLE II. Orientation angle θ, ϕ, value of the angular momentum and ratio of reduced transition probabilities for different confifurations in ^{188}Ir as calculated by 3D-TAC model.

$\hbar\omega$(MeV)	θ	ϕ	J	$B(M1)/B(E2)$
		$\pi h_{9/2}\otimes\nu i_{13/2}$		
0.200	60.9	0.0	10.7	1.93
0.250	66.0	39.0	12.4	0.83
0.275	68.6	48.0	13.5	0.65
0.300	71.1	54.8	14.7	0.58
0.325	73.7	60.8	16.7	0.38
0.350	77.9	69.0	19.7	0.28
0.375	83.9	76.5	24.7	0.15
		$\pi h_{11/2}\otimes\nu i_{13/2}$		
0.200	55.3	89.5	8.5	20.0
0.250	74.0	89.5	9.5	19.4
0.275	79.6	90.0	25.6	0.22

of the quasiproton and the quasineutron angular momenta. With an increase of the total spin the Coriolis interaction will force the total angular momentum to align on a principle plane and finally along a principal axis, resulting in normal principal axis rotation, and both the broken chiral and signature symmetries will be restored [31]. It should be noted that the calculations yield a chiral solution for the $\pi h_{9/2}\otimes\nu i_{13/2}$ configuration in ^{188}Ir, while such a solution cannot be found for the lighter Ir nuclei.

Within the 3D-TAC model [30] we have also calculated reduced transition probabilities in rotational bands with different configurations. The theoretical values for the $\pi h_{9/2}\otimes\nu i_{13/2}$ and the $\pi h_{11/2}\otimes\nu i_{13/2}$ configurations are presented in Fig. 11 together with experimental results for bands 1 and 2. The experimental $B(M1)/B(E2)$ ratios for band 1 show some signature dependence, which cannot be taken into account in the 3D-TAC approach. Since the signature is not a good quantum number in 3D-TAC model, the both $\Delta I=2$ se-

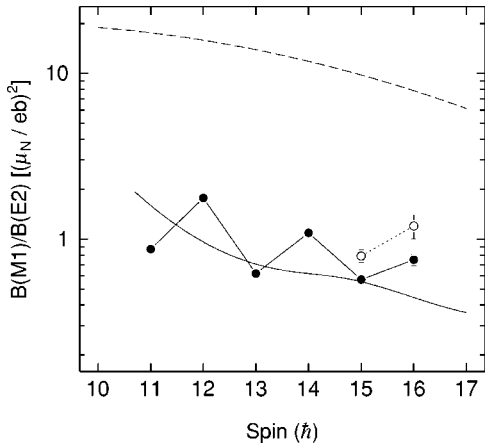

FIG. 11. Experimental $B(M1)/B(E2)$ ratios for band 1 (full circles) and band 2 (open circles) in ^{188}Ir, compared to theoretical calculations within the 3D-TAC model for the $\pi h_{9/2}\otimes\nu i_{13/2}$ (solid line) and the $\pi h_{11/2}\otimes\nu i_{13/2}$ configuration (dashed line).

quences in band 1 are indistinguishable. Nevertheless, it is clear that the calculated average values for the $\pi h_{9/2} \otimes \nu i_{13/2}$ configuration are of the order of the experimental values, while those that are predicted for the $\pi h_{11/2} \otimes \nu i_{13/2}$ configuration differ by an order of magnitude. This strongly supports the suggestion that the yrast band in ^{188}Ir has the $\pi h_{9/2} \otimes \nu i_{13/2}$ configuration. The $\pi i_{13/2} \otimes \nu i_{13/2}$ configuration should also be excluded for this band, because it is expected to lie higher in excitation energy. Figure 11 also shows that the experimental $B(M1)/B(E2)$ values for band 2 are of the same order as the values in band 1 and have the same staggered phase. This supports the suggestions for a common underlying structure for these two sequences.

The initial difference in the excitation energies of bands 1 and 2 is about 200 keV. Figure 6 shows that this difference decreases when the spin increases and at spin $15\hbar$ both bands are degenerate. This situation resembles the experimental observations, which were reported for the chiral doublets in ^{134}Pr and ^{136}Pm nuclei [5,11]. The initial displacement of the chiral bands was attributed to the so called "chiral vibration" (see Ref. [5]). When the triaxial core deformation is not stable at $\gamma=-30°$ the total angular momentum of the system **I** is not constrained to the one of the left- and right-handed systems of different chirality, and can oscillate from one system to the other. However, in Ref. [32] it was shown that even in the ideal case of rigid triaxiality the two chiral bands are separated in energy at low spins.

For axially symmetric odd-odd nuclei, the favorite signature of a rotational band is given as, $\alpha_f=\frac{1}{2}[(-1)^{(j_\pi-1/2)}+(-1)^{(j_\nu-1/2)}]$, where the total angular momentum I is related to α_f by $I=\alpha_f+2n$ $(n=0,1,2,3,\ldots)$. For the $\pi h_{9/2} \otimes \nu i_{13/2}$ configuration $\alpha_f=1$, and the favorite signature band members have odd spin. According to Ref. [1], in an ideal case, aplanar rotation implies breaking of signature symmetry and the disappearance of signature splitting. Experimentally signature splitting is quantified by the energy staggering $S(I)=E(I)-[E(I+1)+E(I-1)]/2$. Since the signature is not conserved quantum number in case of nuclear rotation axis outside any of the principle planes, it is more appropriate to talk that $S(I)$ has odd/even spin dependence. The calculation within the two-particle-plus-rotor model performed in Ref. [32] show the typical behavior of the quantity $S(I)$ in case of the chiral rotation. At the beginning of the chiral band $S(I)$ exhibit odd/even spin staggering, which diminish when the spin increases and finally $S(I)$ takes constant value.

In Fig. 7 $S(I)$ is plotted for the $\pi h_{9/2} \otimes \nu i_{13/2}$ yrast configuration in the odd-odd $^{182-188}$Ir. In comparison with $^{182-186}$Ir, where $S(I)$ odd/even spin staggering increases with spin, in ^{188}Ir $S(I)$ odd/even spin staggering stays constant and even decreases a little in the spin interval of the observation of band 1. This agrees with interpretation of bands 1 and 2 as chiral doublet and calculations made in Ref. [32]. Since we do not observe that the $S(I)$ odd/even spin staggering converges to a constant value, the chiral region of band 1 was not reached in our experiment. The reason for this are the competing single particle states which become more yrast than the levels of bands 1 and 2, when the spin increases.

A different interpretation, that band 2 is a γ-vibrational state coupled to the $\pi h_{9/2} \otimes \nu i_{13/2}$ configuration is rather unlikely, since such excitations lie at about 600 keV for the neighboring even-even nuclei [33], while the excitation of band 2 is $\sim$200 keV with respect to the yrast band. It should be noted, here, that a recent calculation, which has been done within the framework of the interacting boson fermion-fermion model for the mass $A=130$ nucleus ^{134}Pr, suggests that the γ vibration coupled to the $\nu h_{11/2} \otimes \pi h_{11/2}$ configuration comes down in energy as compared to the neighboring even-even nuclei [34]. On the other hand, a very detailed analysis performed in Refs. [13,35] including investigation of nuclear wave functions and electromagnetic properties of the twin bands in ^{128,130,132,134}Cs and ^{132}La nuclei, definitely shows the chiral nature of these bands.

IV. CONCLUSIONS

In summary, we have studied the high-spin structure of ^{188}Ir and extended the levels scheme considerably compare to the previous studies. We observe a pair of $\Delta I=1$ bands which have the same parity and lie above the previously reported $923.7+x$ keV $T_{1/2}=4.2(2)$ ms isomer. Both bands have been assigned $\pi h_{9/2} \otimes \nu i_{13/2}$ configuration, based on the systematics of $\pi h_{9/2}$ and $\pi h_{11/2}$ configurations in neighboring odd-A Ir nuclei and comparison between calculated and experimental $B(M1)/B(E2)$ ratios for $\pi h_{9/2} \otimes \nu i_{13/2}$ and $\pi h_{11/2} \otimes \nu i_{13/2}$ configurations. These two bands are suggested to be a chiral doublet on the base of their experimental features and the 3D-TAC calculations which show existence of chiral rotation in ^{188}Ir. Another possibility for band 2, to be a γ vibration coupled to the $\pi h_{9/2} \otimes \nu i_{13/2}$ configuration was ruled out, because γ vibrational bands in neighboring even-even nuclei has higher excitation energy compare to what we observed experimentally.

ACKNOWLEDGMENTS

This work is supported by the U.S. Department of Energy under Grant Nos. DE-FG02-96ER40983 (University of Tennessee), DE-FG02-91ER-40609 (Yale University), DE-FG02-88ER-40417 (Clark University). D.L.B. also acknowledges partial support of the Bulgarian National Science Fond through Contract No. F-908 and NATO CLG No. 978799. The authors are also grateful to Dr. M. Riley for providing the ^{186}W targets and to Dr. F. Dönau, Dr. V. I. Dimitrov, and Dr. S. Frauendorf for the inspiring discussions.

[1] S. Frauendorf and J. Meng, Nucl. Phys. **A617**, 131 (1997).
[2] S. Frauendorf, Nucl. Phys. **A557**, 259c (1993).
[3] V. I. Dimitrov, S. Frauendorf, and F. Dönau, Phys. Rev. Lett. **84**, 5732 (2000).
[4] S. Frauendorf, Rev. Mod. Phys. **73**, 463 (2001).
[5] K. Starosta *et al.*, Phys. Rev. Lett. **86**, 971 (2001).
[6] J. Meyer-ter-Vehn, Nucl. Phys. **A249**, 111 (1975).
[7] A. Bohr and B. Mottelsson, *Nuclear Structure* (Benjamin, New York, 1975).
[8] C. M. Petrache, D. Bazzacco, S. Lunardi, C. Rossi Alvarez, G. de Angelis, M. de Poli, D. Bucurescu, C. A. Ur, P. B. Semmes, and R. Wyss, Nucl. Phys. **A597**, 106 (1996).
[9] A. A. Hecht *et al.*, Phys. Rev. C **63**, 051302(R) (2001).
[10] T. Koike, K. Starosta, C. J. Chiara, D. B. Fossan, and D. R. LaFosse, Phys. Rev. C **63**, 061304(R) (2001).
[11] D. J. Hartley *et al.*, Phys. Rev. C **64**, 031304(R) (2001).
[12] R. A. Bark, A. M. Baxter, A. P. Byrne, G. D. Dracoulis, T. Kibedi, T. R. McGoram, and S. M. Mullins, Nucl. Phys. **A691**, 577 (2001).
[13] T. Koike, K. Starosta, C. J. Chiara, D. B. Fossan, and D. R. LaFosse, Phys. Rev. C **67**, 044319 (2003).
[14] G. I. Rainovski *et al.*, Phys. Rev. C **68**, 024318 (2003).
[15] C. Vaman, D. B. Fossan, T. Koike, K. Starosta, I. Y. Lee, and A. O. Macchiavelli, Phys. Rev. Lett. **92**, 032501 (2004).
[16] K. Starosta, T. Koike, C. J. Chiara, D. B. Fossan, and D. R. LaFosse, Nucl. Phys. **A682**, 375c (2001).
[17] Th. Hilberath *et al.*, Z. Phys. A **342**, 1 (1992).
[18] G. Seewald, E. Hagn, B. Hinfurtner, E. Zech, D. Forkel-Wirth, R. Eder, and ISOLDE Collaboration, Phys. Rev. Lett. **77**, 5016 (1996).
[19] C. W. Beausang *et al.*, Nucl. Instrum. Methods Phys. Res. A **452**, 431 (2000).
[20] D. C. Radford, Nucl. Instrum. Methods Phys. Res. A **361**, 297 (1995); http://radware.phy.ornl.gov
[21] A. J. Kreiner, C. A. Arias, M. Debray, D. Digregorio, A. Pacheco, J. Davidson, and M. Davidson, Nucl. Phys. **A425**, 397 (1984).
[22] R. Eder, E. Hagn, and E. Zech, Phys. Rev. C **32**, 582 (1985).
[23] P. Kemnitz, L. Funke, H. Sodan, E. Will, and G. Winter, Nucl. Phys. **A245**, 221 (1975).
[24] A. Krämer-Flecken, T. Morek, R. M. Lieder, W. Gast, G. Hebbinghaus, H. M. Jager, and W. Urban, Nucl. Instrum. Methods Phys. Res. A **275**, 333 (1989).
[25] E. Hagn, H. Kleebauer, and E. Zech, Phys. Lett. **104B**, 365 (1981).
[26] A. J. Kreiner, J. Davidson, M. Davidson, P. Thieberger, E. K. Warburton, S. Andre, and J. Genevey, Nucl. Phys. **A489**, 525 (1988).
[27] M. A. Cardona *et al.*, Phys. Rev. C **55**, 144 (1997).
[28] A. V. Afanasjev *et al.*, Phys. Rep. **322**, 1 (1999).
[29] N. I. Nikolov *et al.* (unpublished).
[30] V. I. Dimitrov, F. Dönau, and S. Frauendorf, Phys. Rev. C **62**, 024315 (2000).
[31] F. Dönau, J. Y. Zhang, and L. L. Riedinger, Phys. Lett. B **450**, 313 (1999).
[32] T. Koike, K. Starosta, C. Vaman, T. Ahn, D. B. Fossan, R. M. Clark, M. Cromaz, I. Y. Lee, and A. O. Macchiavelli, in *Frontiers of Nuclear Structure*, edited by P. Fallon and R. Clark, AIP Conf. Proc. No. 656 (AIP, New York, 2003), p. 160.
[33] R. B. Firestone and V. S. Shirley, *Table of Isotopes*, 8th ed. (Wiley, New York, 1978).
[34] S. Brant, D. Vretenar, and A. Ventura, Phys. Rev. C **69**, 017304 (2004).
[35] K. Starosta, C. J. Chiara, D. B. Fossan, T. Koike, T. T. S. Kuo, D. R. LaFosse, S. G. Rohoziński, Ch. Droste, T. Morek, and J. Srebrny, Phys. Rev. C **65**, 044328 (2002).